9-2011

Deletion of Rb Accelerates Pancreatic Carcinogenesis by Oncogenic Kras and Impairs Senescence in Pre-Malignant Lesions

Catherine Carrière
Dartmouth College

A. Jesse Gore
Dartmouth College

Alixanna M. Norris
Dartmouth College

Jason R. Gunn
Dartmouth College

Alison Young
Dartmouth College

See next page for additional authors

BASIC AND TRANSLATIONAL—PANCREAS

Deletion of *Rb* Accelerates Pancreatic Carcinogenesis by Oncogenic Kras and Impairs Senescence in Premalignant Lesions

CATHERINE CARRIÈRE,[*,‡] A. JESSE GORE,[*,‡] ALIXANNA M. NORRIS,[*,‡] JASON R. GUNN,[*,‡] ALISON L. YOUNG,[*,‡] DANIEL S. LONGNECKER,[§] and MURRAY KORC[*,‡]

[*]Department of Medicine, Department of Pharmacology, and Toxicology, and [§]Department of Pathology, Dartmouth Medical School, Hanover, New Hampshire; and [‡]Norris Cotton Comprehensive Cancer Center at Dartmouth Hitchcock Medical Center, Lebanon, New Hampshire

See Covering the Cover synopsis on page 785.

BACKGROUND & AIMS: *Rb1* encodes a cell-cycle regulator that is functionally disrupted in most human cancers. Pancreatic ductal adenocarcinomas (PDACs) have a high frequency of mutations in *KRAS* and *INK4A/CDKN2A* that might allow cells to bypass the regulatory actions of retinoblastoma (RB). To determine the role of loss of RB function in PDAC progression, we investigated the effects of *Rb* disruption during pancreatic malignant transformation initiated by oncogenic Kras. **METHODS:** We generated mice with pancreas-specific disruption of *Rb*, in the absence or presence of oncogenic Kras, to examine the role of RB in pancreatic carcinogenesis. **RESULTS:** In the presence of oncogenic Kras, loss of Rb from the pancreatic epithelium accelerated formation of pancreatic intraepithelial neoplasia (PanIN), increased the frequency of cystic neoplasms, and promoted rapid progression toward PDAC. Early stage cancers were characterized by acute pancreatic inflammation, associated with up-regulation of proinflammatory cytokines within the pancreas. Despite the presence of markers associated with oncogene-induced senescence, low-grade PanIN were highly proliferative and expressed high levels of p53. Pancreatic cancer cell lines derived from these mice expressed high levels of cytokines, and transcriptional activity of p53 was impaired. **CONCLUSIONS: *Rb* encodes a tumor suppressor that attenuates progression of oncogenic Kras-induced carcinogenesis in the pancreas by mediating the senescence response and promoting activity of the tumor suppressor p53.**

Keywords: Proliferation; Transformation; Signaling; Chemokine.

Pancreatic ductal adenocarcinoma (PDAC) is the fourth leading cause of cancer-related death in the United States.[1] PDAC arises from precursor lesions, predominantly pancreatic intraepithelial neoplasia (PanIN), which progress from low grade, PanIN-1A and -1B, to intermediate and high-grade PanIN-2 and -3, respectively.[2]

The biological aggressiveness of PDAC derives from cancer cells that harbor driver mutations in several key genes, including the *KRAS* oncogene (~95%), and the *TP53* (~80%), *SMAD4* (~50%), and *INK4A/CDKN2A* (~85%) tumor-suppressor genes.[3] *INK4A/CDKN2A* encodes $p16^{Ink4a}$, which activates the tumor-suppressive functions of retinoblastoma (RB), a nuclear phosphoprotein encoded by the *RB1* tumor-suppressor gene.[4,5] In PDAC cases in which *INK4A/CDKNA* is not mutated, it is silenced epigenetically.[3] Thus, there is a near-universal loss of $p16^{Ink4a}$ in PDAC. PDAC also is associated with overexpression of multiple tyrosine kinase receptors and their ligands,[6] which, when superimposed on the presence of oncogenic Kras, loss of $p16^{Ink4a}$, and high levels of cyclin D1,[7] could impede RB function. These observations suggest that RB inactivation may be of crucial importance in PDAC.

PDAC mouse models that recapitulated human disease originally were generated by targeting a conditionally mutated *Kras* allele (*LSL-Kras*^{G12D}) to pancreatic progenitors, using *Pdx1* and *Ptf1a* promoters.[8] In these mice, PanIN progresses slowly and at a low frequency toward PDAC by approximately 36 weeks of age. To delineate the role of RB in PDAC, we used $Rb^{LoxP/LoxP}$ ($Rb^{L/L}$) mice[9] to generate compound mutant *Pdx1-Cre;LSL-Kras*^{G12D}*;Rb*$^{L/L}$ (*Rb/K*) mice that carry activated oncogenic Kras and deleted RB in the pancreas. Although RB deletion alone does not alter pancreatic histology, it accelerates the induction of oncogenic Kras-associated neoplasia, and progression to PDAC. In early cancer stages, mice show acute pancreatic inflammation and increased expression of proinflammatory cytokines, produced, in part, by the cancer cells. Low-grade lesions co-express senescence and proliferation markers suggesting that oncogene-induced senescence (OIS) is bypassed. All lesions are highly proliferative and display high levels of wild-type p53, which we show in vitro is

Abbreviations used in this paper: ADM, acinar-to-ductal metaplasia; CK19, cytokeratin 19; IL, interleukin; MCN, mucinous cystic neoplasia; MCP1, monocyte chemotactic protein-1; MDM2, murine double minute-2; OIS, oncogene-induced senescence; PanIN, pancreatic intraepithelial neoplasia; PDAC, pancreatic ductal adenocarcinomas; RB, retinoblastoma; SA-βGal, senescence-associated β-galactosidase; TGF, transforming growth factor.

0016-5085/$36.00
doi:10.1053/j.gastro.2011.05.041

transcriptionally inactive. Thus, loss of RB function in the context of oncogenic Kras leads to a proinflammatory pancreatic microenvironment, impaired OIS and enhanced cell proliferation, and p53 dysfunction, resulting in marked acceleration of pancreatic carcinogenesis.

Materials and Methods

Detailed Materials and Methods are described in the Supplementary Materials and Methods section.

Genetically Modified Mice and Animal Care

Pdx1-Cre and conditional $Rb^{L/L}$ and $LSL\text{-}Kras^{G12D}$ mice were described previously.[8–10] Animal experiments were approved by the Institutional Animal Care and Use Committee at Dartmouth College.

Immunohistochemistry

Mice were perfused with phosphate-buffered saline and then 10% formalin; pancreata then was dissected, fixed overnight, and paraffin-embedded. Immunohistochemistry was performed using standard protocols.

Senescence-Associated β-Galactosidase Staining

Cryosections from *K* and *Rb/K* pancreata were prepared and stained in parallel under exactly the same conditions,[11] yielding highly reproducible results.

Immunoblotting

Immunoblotting was performed as described.[12]

Primary Cell Line Preparation and p53 Mutation Analysis

Primary cell lines were prepared as described.[13] RNA was isolated with the RNeasy Mini kit (Qiagen, Valencia, CA) and complementary DNA (cDNA) was prepared with the Superscript III First Strand cDNA Synthesis Kit (Invitrogen, Carlsbad, CA). Sequencing was performed by the Molecular Biology Core at Dartmouth College (Hanover, NH).

Rb Recombination and $Kras^{G12D}$ *Expression*

Rb recombination[9] and $Kras^{G12D}$ expression were analyzed as described.[14]

Quantitative Reverse-Transcription Polymerase Chain Reaction

Pancreatic RNA was isolated using the low-temperature guanidine isothiocyanate method.[15,16] TaqMan expression assays (Applied Biosystems, Foster City, CA) were performed on cell line and pancreatic cDNA.

Proliferation Assays

Cell growth was monitored as described.[17]

Luciferase Assays

Reporter constructs were transfected into murine primary cell lines using Lipofectamine 2000 (Invitrogen). Luciferase activity was evaluated using the Dual Luciferase Assay kit (Promega, Madison, WI) and an LMaxII microplate reader (Molecular Devices, Sunnyvale, CA).

Results

Rb *Deletion Synergizes With Oncogenic* Kras *to Accelerate Pancreatic Carcinogenesis*

By crossing *Pdx1-Cre* mice[10] with $Rb^{L/L}$ mice,[9] animals carrying a deletion of *Rb* in the pancreatic epithelium, and subsequently in all pancreatic cell types, were generated. These mice were born at the expected frequency, showing approximately 80% efficiency of *Rb* recombination in the pancreas (Supplementary Figure 1*A*), and had an average lifespan. No abnormalities in the pancreatic cytoarchitecture were observed (Supplementary Figure 1*B*). Thus, as in mouse models null for other pancreatic tumor-suppressor genes,[14,18–21] RB inactivation per se does not affect pancreatic development or induce neoplasia.

Although no phenotype was detected at embryonic day 15 and postnatal day 1, as early as postnatal week 1 the pancreatic *Rb* deletion concomitant with $Kras^{G12D}$ (*Rb/K* mice) activation led to the development of high-grade PanIN (Figure 1*A*). By 2 weeks, low and high-grade PanIN (Figure 1*B*) were frequent, often occurring in conjunction with low- and high-grade cystic neoplasms (Figure 1*C* and *D*), and 1 of 5 mice developed PDAC (Figure 1*E*). Nearly 20% of *Rb/K* mice died during the first month of life, displaying severe cachexia and atrophic pancreata. Histologic analysis of 10 such pancreata, collected from moribund mice, showed both low- and high-grade lesions and large cysts, suggesting that these mice were developing PDAC and cystic changes. Overall, *Rb/K* mice had a median survival of approximately 10 weeks (Figure 1*F*). Excluding animals that died during the first month of life and had no necropsy (12 mice) did not significantly alter the Kaplan–Meier survival plot (Figure 1*F*).

In mice expressing oncogenic Kras with *Rb* haploinsufficiency (*Pdx1-Cre*;$LSL\text{-}Kras^{G12D}$;$Rb^{L/+}$, $Rb^{L/+}$/*K* mice) PanIN and cystic neoplasms progressed slowly, and median survival increased to 36 weeks (Figure 1*F* and Table 1). Nonetheless, compared with *Pdx1-Cre*;$LSL\text{-}Kras^{G12D}$ mice (termed *K*), PanIN progression in $Rb^{L/+}$/*K* mice was faster, cyst formation was more common (Supplementary Figure 2), and survival was greatly reduced (Table 1 and Figure 1*F*).[8,14] Although *Pdx1-Cre* also is expressed in the duodenum, only low to moderate dysplasia, manifested by the presence of pseudostratified epithelium and rare luminal mitosis, was observed in the duodenal mucosa of *Rb/K* animals (not shown).

Histologic Characteristics of Pancreatic Lesions in Rb/K *Mice*

Akin to human beings,[22] PanIN in *Rb/K* mice developed in a peripheral location that did not initially involve the main duct or its large branches. These PanIN were cytokeratin 19 (CK19)-positive and accumulated mucins as evidenced by Alcian blue staining (Supplementary Figure 3*A* and *B*). Wnt and Notch signaling pathways were up-regulated, as shown by strong β-catenin and Hes1 immunoreactivity, respectively (Supplementary Figure 3*C*

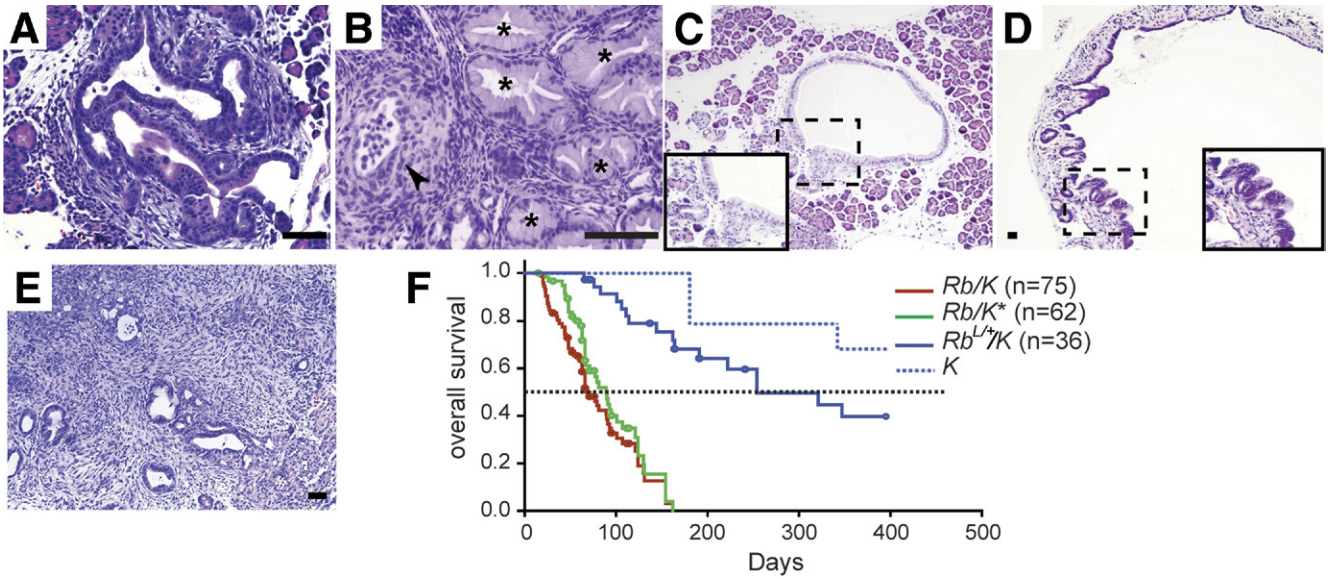

Figure 1. *Rb/K* animals develop early pancreatic lesions. (*A*) One-week-old mouse: PanIN-3. (*B–E*) Two-week-old mice: (*B*) *low-grade and high-grade PanIN with microinvasion (*arrowhead*); (*C*) MCN-like and (*D*) intraductal papillary mucinous neoplasia–like cystic neoplasms; and (*E*) PDAC. (*F*) Kaplan–Meier survival curves: *Rb/K* mice have a shorter lifespan (*red line*) compared with $Rb^{L/+}/K$ (*blue line*) and *K* mice (*dashed blue line*). *Rb/K* survival was similar when mice that died within postnatal month 1 without necropsy were excluded (*green line*). Survival for *K* mice was derived from a previous study.[8] *Scale bars*, 50 μm.

and *D*), and increased Sonic Hedgehog expression also was observed (not shown). *Rb/K* mice frequently developed pancreatic cystic neoplasms (Table 1). Most of these cysts displayed mucin-rich and CK19-positive columnar epithelium (Supplementary Figure 3*A* and *B*) with low- to high-grade dysplasia (Figures 1*C* and 2*A* and *B*), and were surrounded by an ovarian-like stroma with spindle-shaped cells expressing progesterone and estrogen receptors (Figure 2*C* and *D*). Thus, these cysts were similar to mucinous cystic neoplasia (MCN) in human beings.[23,24] The stroma also harbored activated stellate cells that were rich in α-smooth muscle actin (Figure 2*E*). Wnt and Notch pathways also were activated in these MCN-like lesions (Supplementary Figure 3*C* and *D*) and cyclooxygenase 2 was increased (Figure 2*F*).

Three of 40 mice had a single large cyst (~1.0 cm in diameter) in the head of the pancreas, in close proximity to the biliary duct from which it appeared to derive (not shown). These 3 mice displayed papillary epithelium with nuclear stratification, minimal to moderate dysplasia (Figure 1*D*), and stroma devoid of estrogen and progesterone receptors (not shown), reminiscent of intraductal papillary mucinous neoplasia in human beings.[23] In one case, the intraductal papillary mucinous neoplasia–like lesion occurred in conjunction with PanIN-2 and -3, and MCN-like lesions.

Table 1. PDAC Progression in the Absence of 1 or 2 Alleles of Rb

Genotype	ADM	Cysts	PanIN-1	PanIN-2	PanIN-3	PDAC
Pdx1-Cre;LSL-Kras^{G12D};Rb$^{L/L}$						
2–3 wk (n = 5)	5/5	2/5 (1[a])	5/5	1/5	1/5	1/5
1 mo (n = 11)	10/11	6/11 (2,[a] 1[b])	7/11	4/11	3/11	1/11
2 mo (n = 10)	9/10	8/10 (7[a])	10/10	5/10	3/10	3/10
3 mo (n = 13)	11/13	8/13 (6,[a] 1[b])	12/13	8/13	7/13	6/13
4–5 mo (n = 6)	6/6	3/6 (2,[a] 1[b])	6/6	4/6	4/6	4/6
Pdx1-Cre;LSL-Kras^{G12D};Rb$^{L/+}$						
2–3 mo (n = 7)	6/7	3/7	7/7	2/7	0/7	0/7
4–5 mo (n = 10)	10/10	1[b]/10	10/10	4/10	0/10	0/10
6–8 mo (n = 5)	5/5	2/5	5/5	4/5	2/5	1/5
Pdx1-Cre;LSL-Kras^{G12D}						
2 mo (n = 8)	4/8	0/8	4/8	0/8	0/8	0/8
2–4 mo (n = 16)	12/16	2/16	15/16	2/16	1/16	1/16
4–6 mo (n = 19)	13/19	0/19	19/19	2/19	0/19	0/19
6–10 mo (n = 16)	15/16	3/16	16/16	1/16	1/16	1/16

NOTE. None of the cysts observed in Pdx1-Cre;LSL-KrasG12D mice were MCNs.
[a]Cyst diameter between 1 and 5 mm.
[b]Cyst diameter greater than 5 mm.

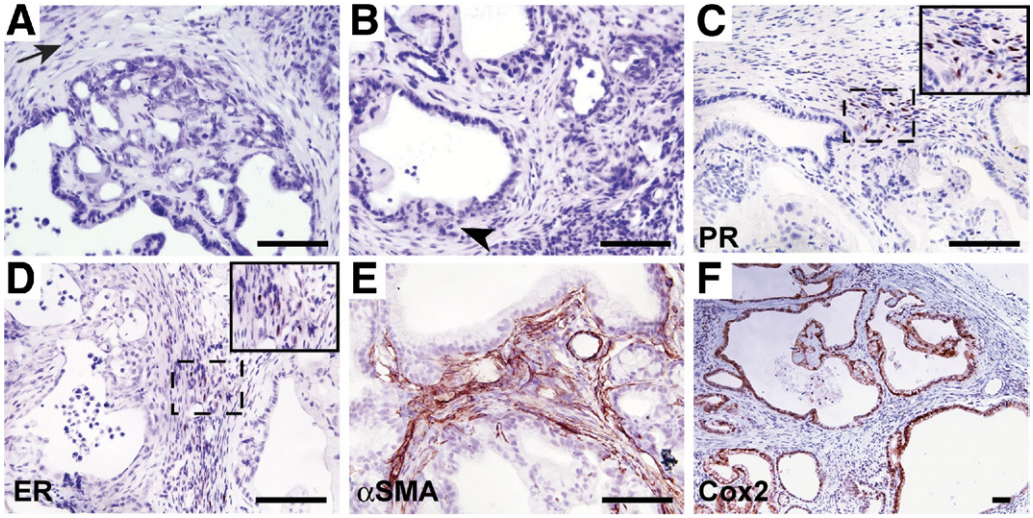

Figure 2. Characteristics of epithelial and stromal compartments of MCN-like lesions. (*A*) Low- to moderate-grade lesions in *Rb/K* mice display disorganized epithelia, without clear nuclear atypia, and are surrounded by hypercellular stroma (*arrow*). (*B*) High-grade lesions display nuclear atypia and loss of basement membrane (*arrowhead*). (*C–E*) Surrounding stroma expresses (*C*) progesterone receptor (PR), (*D*) estrogen receptor (ER), and (*E*) α-smooth muscle actin (α-SMA). (*F*) Lesions overexpress cyclooxygenase 2 (Cox2). *Scale bar*, 50 μm.

PanIN and MCN-Like Lesions in Rb/K *Mice Rapidly Progress to PDAC*

Although normal acinar and ductal cells were not proliferative, there was a marked increase in proliferation in all PanIN in *Rb/K* pancreata: 62.9% ± 2% and 76.7% ± 4% of cells were Ki67-positive in PanIN-1 (Supplementary Figure 3*E*) and PanIN-2/-3, respectively. By contrast, proliferation of low-grade PanIN in *K* mice was only 16% ± 1.8%.[8] In another mouse model, MCN-like lesions showed increased proliferation indices (2%–10%).[20] In *Rb/K* pancreata, however, this figure was 57% ± 2% (Supplementary Figure 3*E*), and foci of acinar-to-ductal metaplasia (ADM) also were proliferative (22% ± 2%). Although RB controls cell proliferation by inhibiting the G1-S transition,[25] these observations suggest that RB attenuates oncogenic Kras-activated mitogenic pathways in the pancreas.

In *Rb/K* mice, invasive PDAC developed with high frequency ranging from 20% (n = 5) at 2 weeks to approximately 70% (n = 6) at 4–5 months. Microinvasion was observed in association with both high-grade PanIN and MCN, as evidenced by basement membrane disruption (Figures 1*B* and 2*B*) and CK19-expressing dysmorphic cells within the adjacent stroma (Supplementary Figure 4*A* and *B*), indicating that both lesions could progress to cancer. Altogether, 14 of 40 *Rb/K* mice developed PDAC (Table 1), which were highly proliferative with a collagen-rich stroma (Supplementary Figure 4*C* and *D*). Thus, aside from the absence of metastases, PDAC in *Rb/K* mice recapitulated many histologic features of human PDAC. $Rb^{L/+}/K$ mice also developed PDAC, but at a very low frequency (1 of 37 after 12 months).

Rb/K *Mice Develop Marked Inflammatory Infiltrates*

Marked inflammatory infiltrates were observed in 1 of 5 pancreata of 1-week-old *Rb/K* mice (not shown), and 3 of 5 pancreata of 2-week-old mice, with occasional foci of ADM (Figure 3*A*). These pancreata showed marked edema with separation of lobules, and harbored many macrophages (Mac3-positive) both near and away from neoplastic lesions (Figure 3*B*). T cells (CD3ϵ-positive) and neutrophils (myeloperoxidase-positive) also were abundant (Figure 3*B*), but B cells were absent (Pax5-negative, not shown). Although inflammatory changes were less frequent by postnatal week 8, some mice still showed inflammatory infiltrates and, occasionally, gross edema (Figure 3*A*). Edematous changes and marked inflammation were never observed at early stages in *K* or $Rb^{L/+}/K$ mice (Supplementary Table 1), suggesting that full inactivation of *Rb* was required to induce the inflammatory reaction.

Cytokine expression was examined next in 3-week-old *Rb/K* pancreata. When compared with littermate controls (including $Rb^{L/L}$ and *Pdx1Cre*;$Rb^{L/L}$), the messenger RNA (mRNA) levels for the proinflammatory cytokines interleukin (IL)-6, IL-1β, tumor necrosis factor-α, CXCL1, CXCL2, and monocyte chemotactic protein-1 (MCP1) were highly increased (Figure 3*C* and *D*). In addition, the immune-modulating growth factors, transforming growth factor (TGF)-β1, -β2, and -β3, were up-regulated in 50%–60% of *Rb/K* pancreata (Figure 3*E*). These cytokines also were increased in *K* pancreata compared with their littermate controls (Figure 3*C–E*), but only at stages at which low-grade lesions (3 months) and pronounced ADM-associated inflammation (6 months) are common (Supplementary Table 1 and Supplementary Figure 2). On average, cytokine levels were similar in *K* and *Rb/K* pancreata. However, one-third to one-sixth of the *Rb/K* mice showed dramatic increases in IL-6, IL-1β, and CXCL2, which correlated with the presence of extensive inflammation histologically (not shown). TGF-β1, -β2, and -β3 levels also were higher in *Rb/K* pancreata.

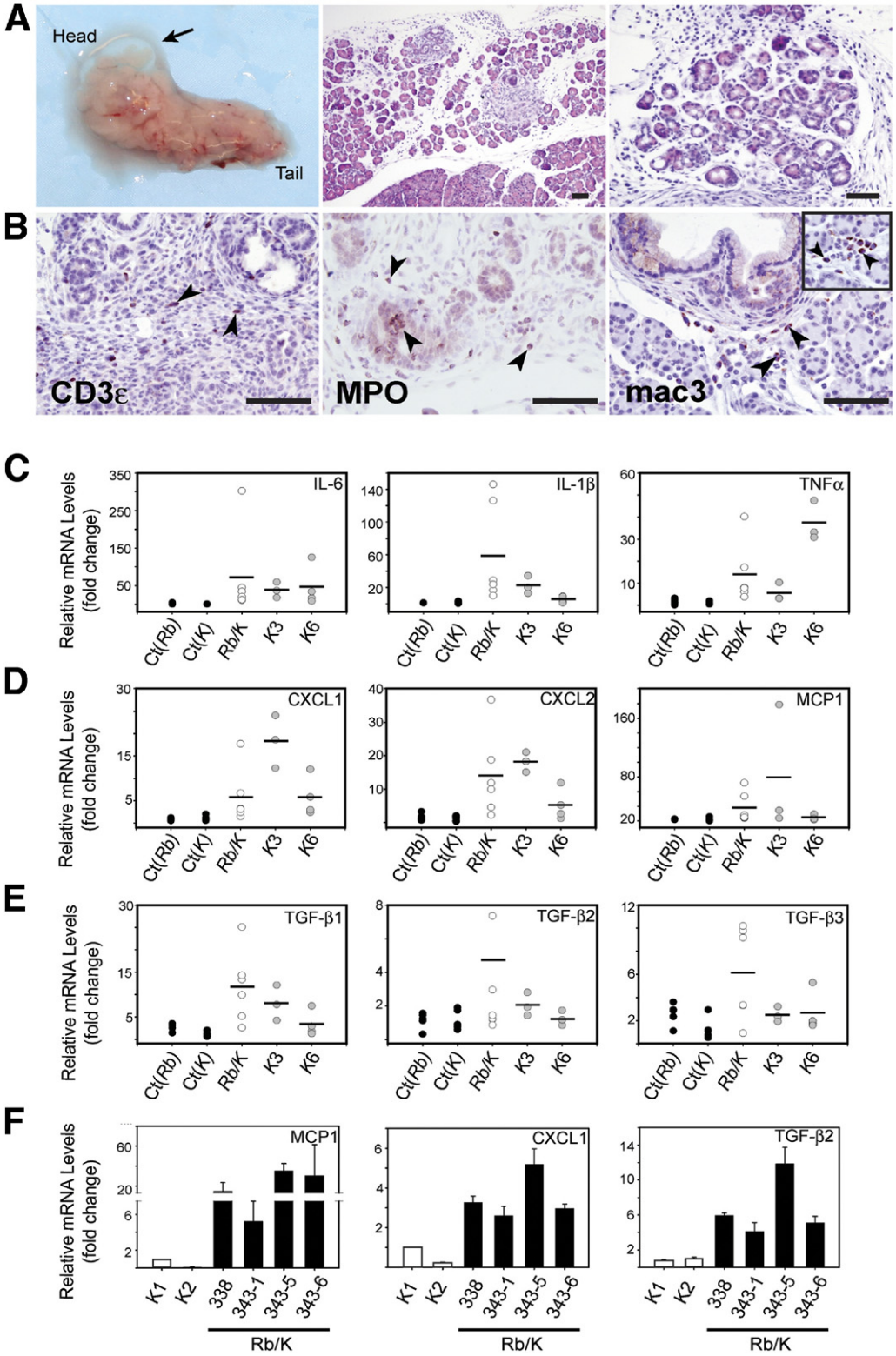

Figure 3. *Rb/K* pancreata display acute pancreatic inflammation. (*A*) Two-month-old mouse (*left panel*): gross edema. (*A* and *B*) Two-week-old mice: (*A*) diffuse (*middle panel*) and focal inflammation around neoplasms and ADM foci (*middle* and *right panels*); (*B*) CD3ε-positive T cells, myeloperoxidase (MPO)-positive neutrophils, and Mac3-positive macrophages adjacent to PanIN, and in normal-appearing pancreas (*inset*). *Scale bar*, 50 μm. (*C–E*) Proinflammatory cytokines are up-regulated in 3-week-old *Rb/K* pancreata (*open circles*), and 3- (*K3*) and 6- (*K6*) month-old *K* mice (*shaded circles*) compared with their littermate controls (*black circles*, Ct(*Rb*) and Ct(*K*)). *Horizontal bars* denote mean expression levels. (*F*) MCP1, CXCL1, and TGF-β2 mRNA levels were increased markedly in all Rb/K (*solid bars*) compared with K cells (*open bars*).

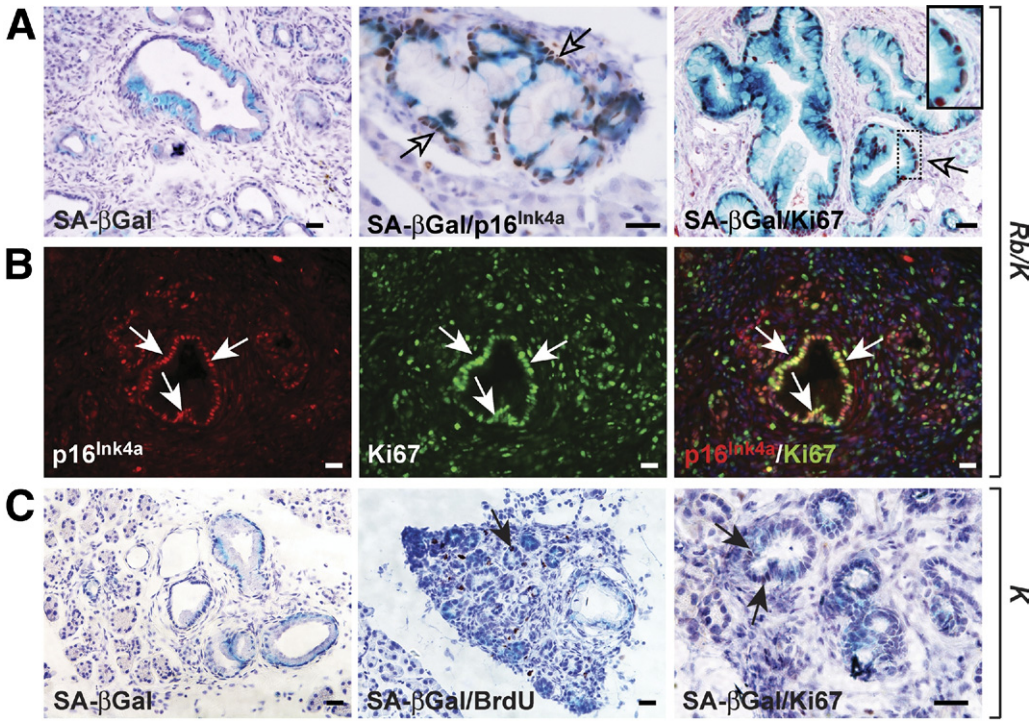

Figure 4. Senescence is bypassed in *Rb/K* pancreata. (*A*) SA-βGal activity (*left panel*) co-localizes (*arrows*) with p16^{Ink4a} (*center panel*) and Ki67 (*right panel*) in low-grade *Rb/K* PanIN. (*B*) Most p16^{Ink4a}-expressing cells (*red*) co-express (*arrows*) Ki67 (*green*) as shown by the overlay (*right panel*). (*C*) In *K* pancreata, low-grade PanIN display SA-βGal activity (*left panel*), but rare bromodeoxyuridine (BrdU) incorporation (*center panel*), and Ki67 expression (*right panel*, *arrows*). *Scale bar*, 50 μm.

To study the possibility that the inflammation was related directly to RB deletion in the cancer cells, 2 primary cell lines were established from 2-month-old *Rb/K* pancreata (Rb/K338 and 343). Several clones (Rb/K343-1 to -6) were isolated from Rb/K343 cells. As controls, we generated cell lines from *K* pancreata (K1 and K2). RB was absent in all Rb/K cell lines (Supplementary Figure 5*A*–*C*) and *Kras*^{G12D} expression was confirmed in all cell lines. Although all cell lines formed tumors in nude mice, except for K2 cells, none were derived from grossly visible tumors, suggesting that they originated from early stage malignancies. All experiments were performed on early passage cells (<12)[8,14,20,21] to minimize alterations in culture. In Rb/K cells, CXCL1, MCP1, and TGF-β2 mRNA levels were increased 4-fold, 5- to 35-fold, and 7-fold, respectively, compared with K 'cells (Figure 3*F*). The levels of TGF-β1, -β3, and other assayed cytokines were similar between *Rb/K* and *K* cells, whereas IL-6 and IL-1β levels were very low in all cell lines.

Rb *Deletion Leads to a Bypass of* Kras^{G12D}-*Induced Senescence*

Ras-associated oncogenic stress can lead to OIS,[26] a process that causes irreversible cell-cycle arrest. Given the involvement of RB in senescence,[27,28] we next examined senescence status in *Rb/K* and *K* pancreata. Senescence-associated β-galactosidase (SA-βGal), an early senescence marker, and p16^{Ink4a}, an essential component of senescence, were detected in PanIN-1 in both *Rb/K* and *K* mice (Figure 4*A*–*C*). Not all PanIN displayed SA-βGal activity, and adjoining cells were always negative, underscoring SA-βGal staining specificity. Dramatically, in *Rb/K* pancreata, SA-βGal- and p16^{Ink4a}-positive PanIN-1 cells were highly proliferative, as evidenced by frequent overlap with Ki67 immunoreactivity (Figure 4*A* and *B*). Indeed, the vast majority of SA-βGal–expressing cells co-expressed Ki67.

By contrast, in *K* pancreata only rare proliferating cells were detected in PanIN-1, and none of them expressed SA-βGal (Figure 4C) or p16^{Ink4a} (not shown). Interestingly, p16^{Ink4a} was increased in all grade PanIN and MCN-like lesions in *Rb/K* mice, but was decreased markedly in proliferating PDAC cells (Supplementary Figure 6*A*–*C*), indicating that p16^{Ink4a} is lost during progression from PanIN-3 to PDAC.

No consistent increases in the expression of the putative senescence markers Dec1 and DcR2 were observed in PanIN-1 in either mouse model, and there were no differences in trimethylated histone K9 immunoreactivity, a marker of heterochromatization (not shown). Given these inconclusive results, microarray studies were performed to compare the expression of senescence-associated genes in Rb/K and K cells. There were highly significant, 10-, 7-, 25-, and 5.3-fold, increases in the mRNA levels encoding p19^{ARF}, insulin-like growth factor binding protein 7, caveolin-1, and p15, respectively, in proliferating Rb/K cells, all of which have been associated with cellular senescence (Supplementary Figure 7).[29–32] These observations suggest that in *Rb/K* mice, senescence is initiated,

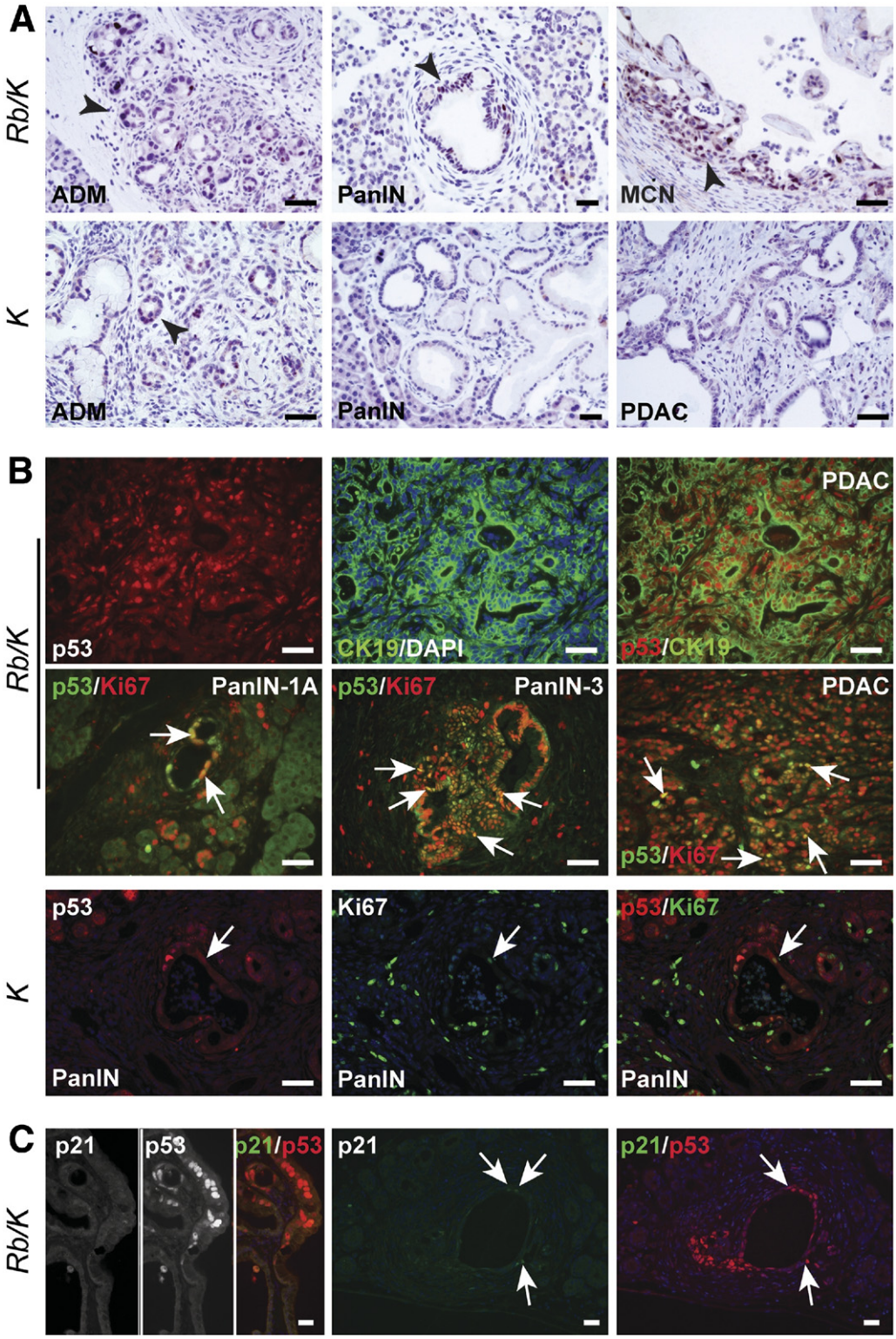

Figure 5. RB loss together with *Kras*^{G12D} activation causes p53 accumulation. (*A*) In *Rb/K* pancreata, p53 (*arrowheads*) is abundant in ADM, PanIN, and MCN-like lesions, but only in ADM foci in *K* pancreata. (*B*) Double immunofluorescence reveals that p53-expressing cells (*red*) are mainly epithelial (CK19-positive; *green*), and are highly proliferative (Ki67-positive; *green*) in low- and high-grade PanIN, and PDAC (*arrows* exemplify co-expression). In *K* pancreata (*lower panels*), p53 expression (*red*) is rare and does not overlap (*arrows*) with Ki67 (*green*). (*C*) p21 expression is very low in lesions and rarely overlaps with p53 (*arrows*). The exposure time for p21 is 3-fold longer than for p53. *Scale bar*, 25 μm.

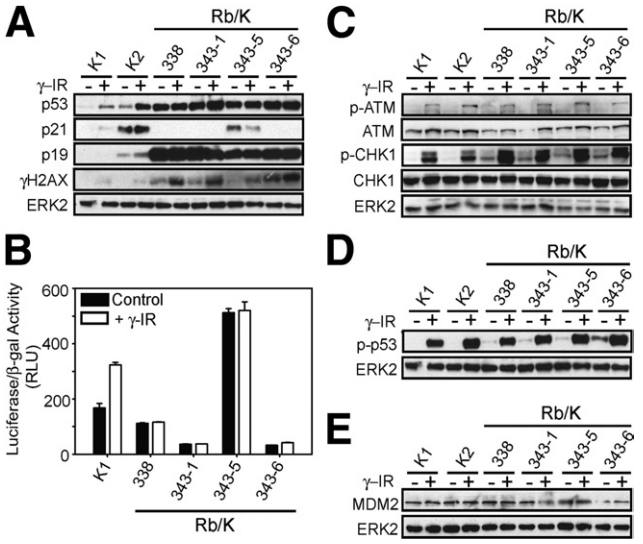

Figure 6. p53 is dysfunctional in Rb/K cells. (*A*) Western blots on Rb/K and K lysates show that p53 and p19^{ARF} are highly increased in Rb/K cells, and p21 is not induced by γ-irradiation in Rb/K cell lines (except Rb/K343-5). After γ-irradiation, γ-H2AX, a DNA damage marker, increases in all cell lines. (*B*) p53 transcriptional activity is very low in Rb/K cell lines except Rb/K343-5. (*C*) DNA damage response pathways are induced by γ-irradiation in K and Rb/K cells. (*D*) γ-irradiation induced p53 phosphorylation (serine 18). (*E*) MDM2 levels are similar in all cell lines.

but cells do not arrest and, instead, escape senescence and show increased proliferation.

Rb *Deletion in the Presence of Oncogenic Kras Leads to Dysregulation of p53 Function*

p53 is a crucial mediator of senescence and cell-cycle arrest that is activated in response to diverse cellular stresses.[33–35] Therefore, we evaluated p53 expression in *Rb/K* and *K* pancreata, and in derived cell lines. Strong nuclear p53 immunoreactivity was present in all lesions (Figure 5*A*) and PDAC (Figure 5*B*) in *Rb/K* pancreata, frequently overlapping with Ki67 (Figure 5*B*). By contrast, *K* pancreata had significantly less p53-positive cells (Supplementary Figure 8*A*), where it primarily was confined to nonproliferative ADM foci and stromal cells (Figure 5*A* and *B*). p21$^{CIP1/WAF1}$ (p21), a key p53 target that elicits growth inhibition and a senescence response,[36] was present at very low levels in *Rb/K* pancreata, infrequently in neoplastic cells, and, rarely, co-localizing with p53 (Figure 5*C*), suggesting that the low levels of p21 in *Rb/K* pancreata derived through p53-independent mechanisms.[37,38]

To further delineate p53 dysregulation in *Rb/K* pancreata, p53 and p21 expression was examined in Rb/K cell lines. Despite high p53 levels, p21 mRNA levels were decreased markedly in Rb/K cells (Supplementary Figure 8*B*), and p21 protein was evident in only one cell line (Rb/K343-5; Figure 6*A*). After DNA damage induction by γ-irradiation, the expected increase in p53 and p21 was seen in K, but not Rb/K cells (Figure 6*A*). Low p21 levels in the face of high p53 suggested that p53 might be transcriptionally inactive. Indeed, with the exception of Rb/K343-5, all Rb/K cell lines had low basal p53 transcriptional activity, which failed to increase after γ-irradiation, whereas K1 cells showed increased activity (Figure 6*B*). None of the 7 Rb/K cell lines harbored a mutated p53 gene, as determined by cDNA sequencing. It was important, therefore, to confirm the loss of p53 transcriptional activity. Accordingly, we assessed the expression levels of several p53 target genes in Rb/K cells, including p21, murine double minute-2 (Mdm2), and pro-apoptotic and pro-survival genes, many of which were down-regulated significantly (Supplementary Figure 8*B–D*).

To determine whether the DNA damage response pathways that activate p53 were functional, we next examined γH2AX, phospho-ATM (S1981), and phospho-CHK1 (S345) expression after γ-irradiation. After irradiation all 3 markers were increased in Rb/K and K cells (Figure 6*A* and *C*), in conjunction with increased phosphorylation of p53 on Ser18 (Figure 6*D*). Thus, Rb/K and K cells maintained an intact DNA damage response upstream of p53.[34]

We next compared p53 turnover in K and Rb/K cells. In K cells, activated p53 protein was below the level of detection within 45 minutes of cycloheximide (2 μg/mL) addition, whereas in Rb/K cells the p53 levels remained markedly increased even after a 6-hour incubation with 10 μg/mL cycloheximide (not shown), underscoring the marked p53 stability in Rb/K cells. Because p19^{ARF} is a major regulator of p53 protein stability, preventing Mdm2 from targeting p53 for degradation, we next compared the expression of p19^{ARF} and Mdm2 in these cells. Although Mdm2 levels were similar in Rb/K and K cells at the protein and RNA levels (Figure 6*E* and Supplementary Figure 8*B*), in congruence with the array results (Supplementary Figure 7), p19^{ARF} was increased in Rb/K cells (Figure 6*A*). Thus, given the normal p53 mRNA levels (Supplementary Figure 8*E*), p53 accumulation in Rb/K cells could be explained by p19^{ARF}-mediated sequestration of Mdm2 and subsequent p53 protein stabilization.

The loss of p53 transcriptional activity suggested that p53-dependent DNA repair mechanisms also could be altered in Rb/K cells, potentially leading to chromosomal instability. Moreover, impaired p53 function has been reported to lead to chromosomal instability in another PDAC model.[21] All Rb/K cell lines displayed an increased number of centrosomes and aberrant spindle formation in mitotic cells whereas none of the K cells showed more than 2 centrosomes in any mitotic cell (Supplementary Figure 9*A*). Abnormal mitotic events also were observed in advanced PDAC in Rb/K pancreata (Supplementary Figure 9*A*). Moreover, spectral karyotyping analysis showed that Rb/K cells had major chromosomal disruption, including amplification and translocation, and the presence of centric fragments (Supplementary Figure 9*B*). Thus, in the presence of oncogenic Kras, RB loss leads to chromosomal instability.

Discussion

A crucial feature of neoplastic transformation is loss of cell-cycle control. Active, hypophosphorylated RB is a key tumor suppressor that prevents cell-cycle progression,[39,40] and alterations in the RB pathway have been identified in nearly every human malignancy.[41] Multiple pathways regulate RB phosphorylation and modulate its activity.[42] Although the presence of oncogenic Kras could inactivate RB and enhance transformation, in some cell types, ras-induced oncogenic transformation requires RB.[43] Given these divergent possibilities, and the need to assess the role of RB in PDAC, we examined the consequence of *Rb* deletion on Kras-induced pancreatic carcinogenesis.

In this study, RB inactivation alone did not affect pancreas development, and it did not induce pancreatic neoplastic transformation. However, concomitant Kras activation resulted in rapid development of PanIN and MCN-like cystic papillary neoplasms, which occurred in conjunction with marked pancreatic inflammation, pancreatic atrophy, rapid progression to PDAC at a high frequency, and a median survival of 10 weeks. Thus, *Rb/K* mice show one of the most lethal phenotypes of all PDAC mouse models,[8,14,18–21,44] underscoring the tumor-suppressive role of RB in the pancreas. $Rb^{L/+}/K$ animals also displayed accelerated lesion progression and decreased survival. However, there was rare progression to PDAC, indicating that loss of both *Rb* alleles, and therefore full inactivation, is required to maximally promote Kras-driven oncogenesis. Signaling pathways that have been reported as being activated in human PanIN, such as Wnt, Notch, and Sonic Hedgehog, were up-regulated in PanIN and MCN-like neoplasms in *Rb/K* mice**,** underscoring the relevance of the *Rb/K* model to human PDAC. Moreover, MCN previously was characterized in only 1 mouse model.[19] Thus, *Rb/K* mice also would allow for improved studies of the pathobiology of MCN.

The acute inflammation in *Rb/K* mice was associated with increased expression of proinflammatory cytokines, including IL-6, which helps recruit neutrophils and facilitates Kras-mediated neoplastic transformation in various cell types by promoting cell survival,[45] and IL-1β and tumor necrosis factor-α, which contribute to neutrophil activation.[46] These cytokines also were expressed at high levels in *K* pancreata, but only in older mice, and they were never associated with edematous changes, as observed in 1-month-old *Rb/K* pancreata. Moreover, only Rb/K cells expressed high levels of CXCL1, TGF-β2, and MCP-1. CXCL1 and TGF-βs are neutrophil chemoattractants,[46] and MCP1, which also is produced by injured acinar cells during the early stages of acute pancreatitis, is a potent monocyte chemoattractant.[47] Thus, Rb/K cells produce and potentially release proinflammatory cytokines, a hallmark of an SA secretory phenotype.[48,49] These findings suggest that in *Rb/K* mice, transformed cells produce high levels of chemokines that recruit inflammatory cells, and induce a highly proinflammatory microenvironment, leading to the observed pancreatitis-like changes and abundant inflammation.

We and others have shown that acute and chronic pancreatitis promote cancer progression in oncogenic Kras-driven PDAC mouse models.[50–53] Moreover, inflammation and neoplastic transformation often appeared concomitantly in *Rb/K* mice, suggesting that these processes were interdependent. Given the importance of inflammation in cancer progression, *Rb/K* mice are an excellent model for investigating the relationship between oncogenic Kras, pancreatic inflammation, and PDAC initiation and progression.

Just as low-grade PanIN in *Rb/K* pancreata showed senescence markers ($p16^{Ink4a}$ and SA-βGal) and enhanced proliferation, proliferating Rb/K cells displayed activation of a senescence program, evidenced by increased $p19^{ARF}$, insulin-like growth factor binding protein 7, caveolin-1, and p15 expression. Increased expression of $p19^{Arf}$ most likely was owing to deregulated E2F activity in the absence of RB, which could sequester Mdm2 and impede p53 degradation.[54] Moreover, in Rb/K cells, p53 was phosphorylated on Ser18 in the absence of exogenous stress and caveolin-1 was overexpressed, and both alterations disrupt p53:Mdm2 interactions.[29,55] These observations may explain why Rb/K cells showed increased p53 protein levels but normal p53 RNA levels.

Despite high p53 levels in Rb/K cells, and the absence of mutations in its coding region, p53 was dysfunctional and could neither enforce senescence nor suppress proliferation. Several lines of evidence support this conclusion, and indicate that these perturbations also were present in *Rb/K* pancreata. First, p53 did not activate transcription in a reporter assay, and analysis of a panel of p53 target genes showed that several classes of these genes were down-regulated in Rb/K cells. Second, Rb/K cells showed chromosomal instability, consistent with defective DNA repair observed in the absence of functional p53. Third, p21 expression was attenuated markedly in *Rb/K* lesions and rarely co-localized with p53, which correlated with low, uninducible p21 expression in vitro. By contrast, in fibroblasts, RB loss up-regulates p21, which cooperates with $p16^{Ink4a}$ to preserve oncogenic ras-induced senescence.[28] Silencing of p21 in these cells induces senescence bypass that is not compensated for by the RB family members, p107/p130.[28] Thus, it is likely that senescence escape in early PanIN lesions in *Rb/K* mice is aborted because of the failure of p53 to up-regulate p21.

It is not clear whether p53 is dysfunctional because of the failure to bind DNA and recruit transcriptional partners, or because of repressive post-translational modifications. Nonetheless, despite the absence of RB and dysfunctional p53, $p16^{Ink4a}$ inactivation still was required for progression to PDAC. Although it generally is assumed that the main role of $p16^{Ink4a}$ is to regulate RB, these data argue that $p16^{Ink4a}$ and RB have unique and independent tumor-suppressor functions.

In summary, our study reveals several previously unappreciated functions of RB in PDAC progression. In the

presence of an activated *Kras*^{G12D} allele, RB prevents neoplastic cells from bypassing senescence and impedes inflammatory alterations that occur as a result of SA secretory phenotype. Moreover, RB promotes p53 functions to attenuate tumor progression. These findings underscore the importance of devising strategies that target RB pathway disruptions[56] in PDAC, and indicate that the *Rb/K* mouse model could be useful for screening drugs designed to activate p53, and/or prevent pancreatic inflammation and cancer progression.

Supplementary Material

Note: To access the supplementary material accompanying this article, visit the online version of *Gastroenterology* at www.gastrojournal.org, and at doi: 10.1053/j.gastro.2011.05.041.

References

1. Jemal A, Siegel R, Xu J, et al. Cancer Statistics. CA Cancer J Clin 2010.
2. Hruban RH, Adsay NV, Albores-Saavedra J, et al. Pancreatic intraepithelial neoplasia: a new nomenclature and classification system for pancreatic duct lesions. Am J Surg Pathol 2001;25:579–586.
3. Hansel DE, Kern SE, Hruban RH. Molecular pathogenesis of pancreatic cancer. Annu Rev Genomics Hum Genet 2003;4:237–256.
4. Friend SH, Bernards R, Rogelij S, et al. A human DNA segment with properties of the gene that predisposes to retinoblastoma and osteosarcoma. Nature 1986;323:643–646.
5. Lee WH, Shew JY, Hong FD, et al. The retinoblastoma susceptibility gene encodes a nuclear phosphoprotein associated with DNA binding activity. Nature 1987;329:642–645.
6. Preis M, Korc M. Kinase signaling pathways as targets for intervention in pancreatic cancer. Cancer Biol Ther 2010;9:754–763.
7. Gansauge S, Gansauge F, Ramadani M, et al. Overexpression of cyclin D1 in human pancreatic carcinoma is associated with poor prognosis. Cancer Res 1997;57:1634–1637.
8. Hingorani SR, Petricoin EF, Maitra A, et al. Preinvasive and invasive ductal pancreatic cancer and its early detection in the mouse. Cancer Cell 2003;4:437–450.
9. Marino S, Vooijs M, van der Gulden H, et al. Induction of medulloblastomas in p53-null mutant mice by somatic inactivation of Rb in the external granular layer cells of the cerebellum. Genes Dev 2000;14:994–1004.
10. Gu G, Dubauskaite J, Melton DA. Direct evidence for the pancreatic lineage: NGN3+ cells are islet progenitors and are distinct from duct progenitors. Development 2002;129:2447–2457.
11. Carrière C, Seeley ES, Goetze T, et al. The Nestin progenitor lineage is the compartment of origin for pancreatic intraepithelial neoplasia. Proc Natl Acad Sci U S A 2007;104:4437–4442.
12. Kleeff J, Korc M. Up-regulation of transforming growth factor (TGF)-b receptors by TGF-b1 in COLO-357 cells. J Biol Chem 1998; 273:7495–7500.
13. Seeley ES, Carrière C, Goetze T, et al. Pancreatic cancer and precursor pancreatic intraepithelial neoplasia lesions are devoid of primary cilia. Cancer Res 2009;69:422–430.
14. Aguirre AJ, Bardeesy N, Sinha M, et al. Activated Kras and Ink4a/Arf deficiency cooperate to produce metastatic pancreatic ductal adenocarcinoma. Genes Dev 2003;17:3112–3126.
15. Han JH, Stratowa C, Rutter WJ. Isolation of full-length putative rat lysophospholipase cDNA using improved methods for mRNA isolation and cDNA cloning. Biochemistry 1986;26:1617–1625.
16. Chang S-C, Brannon PM, Korc M. Effects of dietary manganese deficiency on rat pancreatic amylase mRNA levels. J Nutr 1990; 120:1228–1234.
17. Neupane D, Korc M. 14-3-3s Modulates pancreatic cancer cell survival and invasiveness. Clin Cancer Res 2008;14:7614–7623.
18. Bardeesy N, Aguirre AJ, Chu GC, et al. Both p16(Ink4a) and the p19(Arf)-p53 pathway constrain progression of pancreatic adenocarcinoma in the mouse. Proc Natl Acad Sci U S A 2006;103: 5947–5952.
19. Bardeesy N, Cheng KH, Berger JH, et al. Smad4 is dispensable for normal pancreas development yet critical in progression and tumor biology of pancreas cancer. Genes Dev 2006;20:3130–3146.
20. Izeradjene K, Combs C, Best M, et al. Kras(G12D) and Smad4/Dpc4 haploinsufficiency cooperate to induce mucinous cystic neoplasms and invasive adenocarcinoma of the pancreas. Cancer Cell 2007;11:229–243.
21. Hingorani SR, Wang L, Multani AS, et al. Trp53R172H and KrasG12D cooperate to promote chromosomal instability and widely metastatic pancreatic ductal adenocarcinoma in mice. Cancer Cell 2005;7:469–483.
22. Hruban RH, Rustgi AK, Brentnall TA, et al. Pancreatic cancer in mice and man: the Penn Workshop 2004. Cancer Res 2006;66: 14–17.
23. Reddy RP, Smyrk TC, Zapiach M, et al. Pancreatic mucinous cystic neoplasm defined by ovarian stroma: demographics, clinical features, and prevalence of cancer. Clin Gastroenterol Hepatol 2004; 2:1026–1031.
24. Yoshiaki M, Kenichiro U, Hiroki O, et al. Intraductal papillary-mucinous neoplasms and mucinous cystic neoplasms of the pancreas differentiated by ovarian-type stroma. Surgery 2006;140: 448–453.
25. Goodrich DW, Wang NP, Qian YW, et al. The retinoblastoma gene product regulates progression through the G1 phase of the cell cycle. Cell 1991;67:293–302.
26. Serrano M, Lin AW, McCurrach ME, et al. Oncogenic ras provokes premature cell senescence associated with accumulation of p53 and p16INK4a. Cell 1997;88:593–602.
27. Burkhart DL, Sage J. Cellular mechanisms of tumour suppression by the retinoblastoma gene. Nat Rev Cancer 2008;8:671–682.
28. Chicas A, Wang X, Zhang C, et al. Dissecting the unique role of the retinoblastoma tumor suppressor during cellular senescence. Cancer Cell 2010;17:376–387.
29. Bartholomew JN, Volonte D, Galbiati F. Caveolin-1 regulates the antagonistic pleiotropic properties of cellular senescence through a novel Mdm2/p53-mediated pathway. Cancer Res 2009;69: 2878–2886.
30. Collado M, Serrano M. The power and the promise of oncogene-induced senescence markers. Nat Rev Cancer 2006;6:472–476.
31. Wajapeyee N, Serra RW, Zhu X, et al. Oncogenic BRAF induces senescence and apoptosis through pathways mediated by the secreted protein IGFBP7. Cell 2008;132:363–374.
32. Wajapeyee N, Serra RW, Zhu X, et al. Role for IGFBP7 in senescence induction by BRAF. Cell 2010;141:746–747.
33. Farnebo M, Bykov VJN, Wiman KG. The p53 tumor suppressor: a master regulator of diverse cellular processes and therapeutic target in cancer. Biochem Biophys Res Commun 2010;396: 85–89.
34. Meek DW. Tumour suppression by p53: a role for the DNA damage response? Nat Rev Cancer 2009;9:714–723.
35. Oren M. Decision making by p53: life, death and cancer. Cell Death Differ 2003;10:431–442.
36. El-Deiry WS, Harper JW, O'Connor PM, et al. WAF1/CIP1 is induced in p53-mediated G1 arrest and apoptosis. Cancer Res 1994;54:1169–1174.
37. Michieli P, Chedid M, Lin D, et al. Induction of WAF1/CIP1 by a p53-independent pathway. Cancer Res 1994;54:3391–3395.
38. Johnson M, Dimitrov D, Vojta PJ, et al. Evidence for a p53-independent pathway for upregulation of SDI1/CIP1/WAF1/p21 RNA in human cells. Mol Carcinog 1994;11:59–64.

39. Hatakeyama M, Weinberg RA. The role of RB in cell cycle control. Prog Cell Cycle Res 1995;1:9–19.
40. Dyson N. The regulation of E2F by pRB-family proteins. Genes Dev 1998;12:2245–2262.
41. Hanahan D, Weinberg RA. The hallmarks of cancer. Cell 2000; 100:57–70.
42. Takahashi A, Ohtani N, Hara E. Irreversibility of cellular senescence: dual roles of p16INK4a/Rb-pathway in cell cycle control. Cell Division 2007;2:10.
43. Williams JP, Stewart T, Li B, et al. The retinoblastoma protein is required for ras-induced oncogenic transformation. Mol Cell Biol 2006;26:1170–1182.
44. Morton JP, Jamieson NB, Karim SA, et al. LKB1 haploinsufficiency cooperates with Kras to promote pancreatic cancer through suppression of p21-dependent growth arrest. Gastroenterology 2010; 139:586–597.e6.
45. Ancrile B, Lim K-H, Counter CM. Oncogenic Ras-induced secretion of IL6 is required for tumorigenesis. Genes Dev 2007;21:1714–1719.
46. Parekh T, Saxena B, Reibman J, et al. Neutrophil chemotaxis in response to TGF-beta isoforms (TGF-beta 1, TGF-beta 2, TGF-beta 3) is mediated by fibronectin. J Immunol 1994;152:2456–2466.
47. Brady M, Bhatia M, Christmas S, et al. Expression of the chemokines MCP-1/JE and cytokine-induced neutrophil chemoattractant in early acute pancreatitis. Pancreas 2002;25:260–269.
48. Coppe J-P, Patil CK, Rodier F, et al. Senescence-associated secretory phenotypes reveal cell-nonautonomous functions of oncogenic RAS and the p53 tumor suppressor. PLoS Biol 2008;6: e301.
49. Collado M, Gil J, Efeyan A, et al. Tumour biology: senescence in premalignant tumours. Nature 2005;436:642.
50. Carrière C, Young AL, Gunn JR, et al. Acute pancreatitis markedly accelerates pancreatic cancer progression in mice expressing oncogenic Kras. Biochem Biophys Res Commun 2009;382: 561–565.
51. Guerra C, Schuhmacher AJ, Canamero M, et al. Chronic pancreatitis is essential for induction of pancreatic ductal adenocarcinoma by K-Ras oncogenes in adult mice. Cancer Cell 2007;11: 291–302.
52. Ji B, Tsou L, Wang H, et al. Ras activity levels control the development of pancreatic diseases. Gastroenterology 2009;137: 1072–1082, 1082 e1-6.
53. Gidekel Friedlander SY, Chu GC, Snyder EL, et al. Context-dependent transformation of adult pancreatic cells by oncogenic K-Ras. Cancer Cell 2009;16:379–389.
54. Polager S, Ginsberg D. p53 and E2f: partners in life and death. Nat Rev Cancer 2009;9:738–748.
55. Bode AM, Dong Z. Post-translational modification of p53 in tumorigenesis. Nat Rev Cancer 2004;4:793–805.
56. Knudsen ES, Wang JYJ. Targeting the RB-pathway in cancer therapy. Clin Cancer Res 2010;16:1094–1099.

Received October 2, 2010. Accepted May 16, 2011.

Reprint requests

Address requests for reprints to: Murray Korc, MD, Department of Medicine, 1 Medical Center Drive, Lebanon, New Hampshire 03756. e-mail: Murray.Korc@Dartmouth.edu; fax: (603) 650-6122.

Conflicts of interest

The authors disclose no conflicts.

Funding

This research was supported by US Public Health Service grant CA-R37-075059, awarded by the National Cancer Institute (M.K.).